Nanoscale environments associated with bioweathering of a Mg-Fe-pyroxene

Karim Benzerara[†‡], Tae Hyun Yoon[†], Nicolas Menguy[§], Tolek Tyliszczak[¶], and Gordon E. Brown, Jr.[†‖]

[†]Surface and Aqueous Geochemistry Group, Department of Geological and Environmental Sciences, Stanford University, Stanford, CA 94305-2115; [§]Laboratoire de Minéralogie-Cristallographie, Unité Mixte de Recherche, 7590 Centre National de la Recherche Scientifique, and Institut de Physique du Globe de Paris, 4 Place Jussieu, 75252 Paris Cedex, France; [¶]Chemical Sciences Division, Lawrence Berkeley National Laboratory, Berkeley, CA 94720; and [‖]Stanford Synchrotron Radiation Laboratory, Stanford Linear Accelerator Center, 2575 Sand Hill Road, MS 99, Menlo Park, CA 94025

Communicated by W. G. Ernst, Stanford University, Stanford, CA, December 3, 2004 (received for review September 13, 2004)

Microorganisms are believed to create microenvironments leading to reaction products not predictable from equilibrium thermodynamics and to unique biomineral morphologies. Unambiguous evidence for such environments is, however, rare in natural samples. We have used scanning transmission x-ray microscopy and spectromicroscopy at the sub-40-nm scale, coupled with transmission electron microscopy, to examine bioweathering products on a meteoritic Fe-Mg-orthopyroxene colonized by a filamentous microorganism. Our measurements reveal an amorphous Al-rich layer beneath the microorganism, calcium carbonates of unique morphology intimately associated with polysaccharides adjacent to the microorganism, and regions surrounding the microorganism with different iron oxidation states. Our results confirm the presence of different microenvironments at this microorganism–mineral interface and provide unique nanometer-scale views of microbially controlled pyroxene weathering products.

aluminosilicate | biomineralization | geomicrobiology | STXM | Urey reaction

Weathering of silicates at Earth's surface has major impacts on the environment, including the formation of soils and the release of cationic nutrients (e.g., Fe and Mn) necessary for the growth of microorganisms and plants (1). Other released cations, such as Ca and Mg, can form Ca- and/or Mg-carbonates, resulting in sequestration of atmospheric CO_2. This reaction, known as the Urey reaction, has been suggested to control Earth's climate on geological time scales (2, 3). Pyroxenes are among the most abundant silicates contributing to these reactions (4). Abiotic dissolution of pyroxenes has been studied extensively in the laboratory (e.g., see ref. 5), but significant differences relative to dissolution rates measured in the field are still not well understood (4, 6). The dissolution of Fe-containing pyroxenes is even more complex because of the redox chemistry of iron.

The role of microorganisms in the dissolution of silicates and the cycling of Fe has been the focus of many experimental studies (e.g., see ref. 7), some of which have shown that microorganisms can radically modify the dissolution rates of silicates. They are thought to do so by creating microenvironments in which pH and other solution variables can dramatically differ from bulk conditions (8, 9), by producing diverse metal-chelating organic ligands (10), or by promoting metabolic redox reactions (11). The pathways of microbially mediated Fe-silicate dissolution reactions in nature remain, however, largely unexplored, particularly at the nanometer scale. Here we report new results on the effects of a microorganism on the dissolution of an Fe^{2+}-Mg orthopyroxene [$(Mg_{0.75}Fe_{0.23}Ca_{0.01})(Si_{0.99}Al_{0.01})O_3$] that was exposed at Earth's surface for 70 years. Although it may not be broadly representative of weathering environments, this sample from the Tatahouine meteorite, which fell in the southern Tunisian desert in 1931, provides an unusual opportunity to examine biotic reaction pathways in a well known time frame and under defined conditions in an arid environment (12–15). Previous SEM and transmission electron microscopy (TEM) analyses of the same sample (15) showed that some of the fragments were colonized by filamentous microorganisms whose taxonomy remains unknown. Evidence for a biological origin of this filament comes from the carbon, nitrogen, and phosphorus content as discussed in ref. 15. The microorganism is in contact with the orthopyroxene and is bordered by a cluster of nanometer-sized, rod-shaped calcite single crystals. Removal of the calcite crystals showed that the underlying pyroxene surface is pitted, suggesting some causal relationship involving the microorganism, calcite precipitation, and enhanced dissolution of the orthopyroxene. This meteorite fragment was selected for further analysis by using focused ion beam (FIB) milling to prepare an ultrathin (80 nm) cross section through the microorganism, the calcite crystals, and the pyroxene. Scanning transmission x-ray microscopy (STXM) was used to perform high spatial and energy resolution near-edge x-ray absorption fine structure (NEXAFS) spectroscopy at the C K-edge, Al K-edge, and Fe L_3-edge at the microorganism–calcite–pyroxene interface. These methods, in combination with TEM, provide remarkably clear chemical-state-specific images of the same sample areas of the microorganism–mineral interface at sub-40-nm spatial resolution and 0.1–0.3 eV (1 eV = 1.602×10^{-19} J) energy resolution that could not be obtained by a single method.

Materials and Methods

FIB Milling. FIB milling was performed with an FEI Model 200 TEM FIB system at the Université Aix-Marseille III. The FIB lift-out method was used to prepare the sample (see Fig. 4) as described by Heaney *et al.* (16). The area studied by Benzerara *et al.* (12) by SEM (figure 1a in ref. 12) could be easily located by using the imaging capabilities of the FIB. A thin layer of platinum was then deposited on the specimen across the filament and the calcite cluster to protect them during the milling process. The FIB system uses a Ga liquid metal ion source for milling. A 30 kV Ga^+ beam operating at ≈20 nA excavated pyroxene from both sides of the Pt layer to a depth of 5 μm. Before removal of the thin slide, the sample was further thinned to ≈80 nm with a glancing angle beam at much lower beam currents of ≈100 pA. Finally, a line pattern was drawn with the ion beam along the side and bottom edges of the thin section allowing its removal. The ≈15-μm × 5-μm × 80-nm slide was transferred at room pressure with a micromanipulator onto the membrane of a C-coated 200 mesh copper grid.

TEM. TEM observations were carried out on a JEOL 2010F microscope operating at 200 kV and equipped with a field emission gun, a high-resolution Ultra High-Resolution pole piece, and a Gatan GIF 200 energy filter.

Abbreviations: FIB, focused ion beam; NEXAFS, near-edge x-ray absorption fine structure; STXM, scanning transmission x-ray microscopy; TEM, transmission electron microscopy.

[‡]To whom correspondence should be addressed. E-mail: benzerar@stanford.edu.

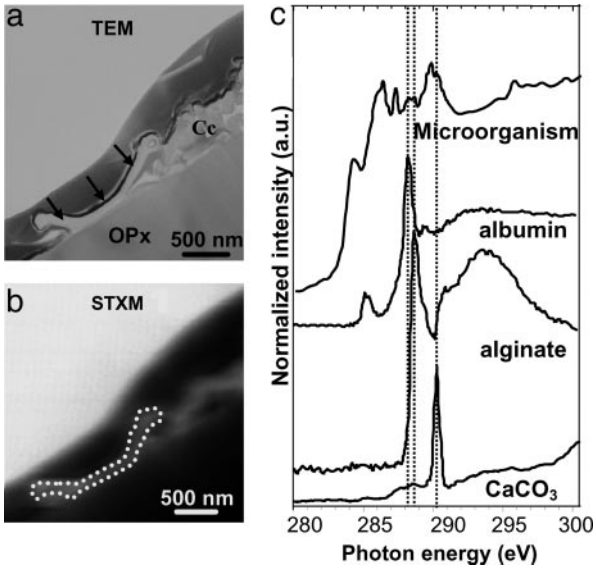

Fig. 1. Spectromicroscopy analysis of filamentous microorganism. (*A*) TEM image of the microorganism (arrows). Cc, calcite cluster; OPx, orthopyroxene. The thin electron-dense layer covering the top of the cross-section is the platinum layer deposited before FIB milling. (*B*) STXM image of the same area at 270 eV. (*C*) C K-edge NEXAFS spectra from the microorganism, and reference calcite and organic molecules (from ref. 19); sodium alginate serves as a model compound for polysaccharide, and albumin serves as a model compound for proteins. Dashed lines at 288.2, 288.6, and 290.2 eV highlight the most prevalent peaks of the model components.

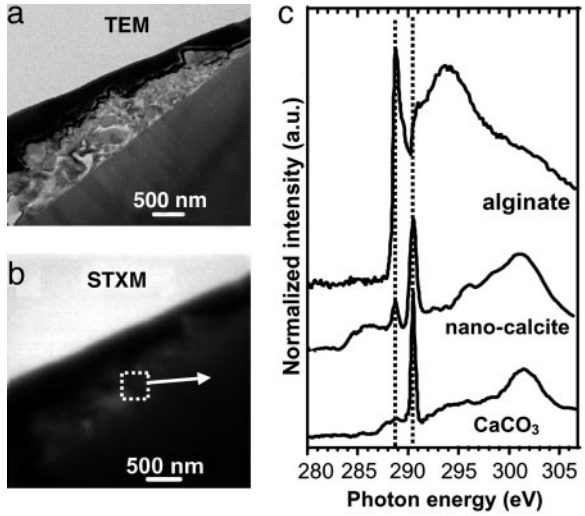

Fig. 2. Spectromicroscopy analysis of the calcite nanocrystals. (*A*) TEM image of the calcite nanocrystal cluster (see ref. 12). (*B*) Equivalent STXM image at 290.3 eV. (*C*) C K-edge NEXAFS spectra from the calcite cluster outlined on *B*, and reference calcite and polysaccharide (sodium alginate) spectra (from ref. 19). Dashed lines at 288.6 and 290.2 eV highlight the mixture of calcite and polysaccharides in the Tatahouine calcite cluster.

STXM. STXM studies were performed at ALS branch line 11.0.2.2 with the synchrotron storage ring operating at 1.9 GeV and 200–400 mA stored current. Technical details about this new branch line and its operation are provided in ref. 17, and recent applications to colloids are presented in ref. 18. Energy calibration was made using the well resolved 3p Rydberg peak at 294.96 eV of gaseous CO_2 for C, the Fe L_3 maximum peak of the Tatahouine pyroxene at 707.8 eV for Fe, and the first major NEXAFS peak of montmorillonite at 1,567.7 eV. The detector used in all measurements reported in this study was a photomultiplier tube with a phosphor scintillator. Stacks of images were obtained by scanning in the *x–y* direction at each energy increment over the energy range of interest (280–320 eV for C, 1,555–1,580 eV for Al, and 705–730 eV for Fe). The contrast results from differential absorption of x-rays, which is dependent on the chemical composition of the sample. Normalization and background correction (in particular the carbon signal from the carbon film of the TEM grid) of the NEXAFS spectra were performed by dividing each spectrum by a second spectrum from a sample-free location on the grid. Spectral and spatial resolutions were <0.1 eV and 40 nm, respectively, at the C K-edge and Fe L_3-edge, and 0.3 eV and 50 nm, respectively, at the Al K-edge. AXIS2000 software (Version 2.1n, A. P. Hitchcock, McMaster University, Hamilton, ON, Canada) was used to align image stacks and extract NEXAFS spectra from image stack measurements.

Results and Discussion

Calcium Immobilization in a Microbial Microenvironment. The C K-edge NEXAFS spectrum of the filament is a complex mixture of peaks (Fig. 1). Comparison with spectra from various biological polymers (19) suggests the presence of polysaccharides (peak at 288.6 eV) and proteins (peak at 288.2 eV) in the filament. Together with the microbial-like morphology of this filament, the presence of nitrogen and phosphorus (15) as well as biochemical compounds, such as proteins, strongly support its biological origin. The peak at 290.2 eV indicates the presence of carbonates on or in the microorganism, suggesting fossilization. C K-edge NEXAFS spectra of reference biological compounds are scarce in the literature and are likely not representative of all C-containing molecules present in this microorganism, which helps explain why several spectral features could not be assigned. Peaks at 284.3 eV, 286.4 eV, and 287.3 eV are thought to be related to C functional groups present in either pristine microbial molecules or molecules resulting from very early diagenesis. The C K-edge NEXAFS spectrum of the calcite crystals is very different from that of the microorganism, showing a major peak at 290.2 eV (Fig. 2), which is characteristic of the π^* resonance of the C═O bond of carbonate groups. An additional peak at 288.6 eV was observed inside the calcite crystal cluster (Fig. 2) and is indicative of carboxyl groups (π^* C═O) likely associated with polysaccharides (19, 20). Many authors have proposed the involvement of organic molecules, either polysaccharides or proteins, in the precipitation of calcium carbonates (e.g., see ref. 21). The nanometer-scale mixture of polysaccharides and carbonates observed on this sample suggests that calcite precipitation occurred in a polysaccharide matrix likely released by the filamentous microorganism. This suggestion is consistent with several previous studies that presented models to explain how polysaccharides could template carbonate precipitation (e.g., see ref. 22). Moreover, the polysaccharides observed in this study help explain the nanometer-sized, rod-shaped calcite crystals found on the Tatahouine meteorite, which is an unusual morphology for calcite crystals (12). Similar unusual morphologies can be achieved when calcite growth occurs in the presence of organic molecules, and polysaccharides in particular (23). Moreover, these calcite crystals are surrounded by an amorphous calcium carbonate layer as shown by high-resolution TEM (12), which is normally highly unstable under natural conditions but can be stabilized in the presence of polysaccharides (24). Both features thus provide potential biosignatures that could be useful in the search for past life in earth and planetary materials. Although some studies have suggested that abiotic dissolution of Mg-silicates could be inhibited in the presence of carbonates (e.g., see ref. 25), SEM and TEM observations on the Tatahouine meteorite have shown that the filamentous microorganism enhanced the dissolution of the pyroxene below the calcite

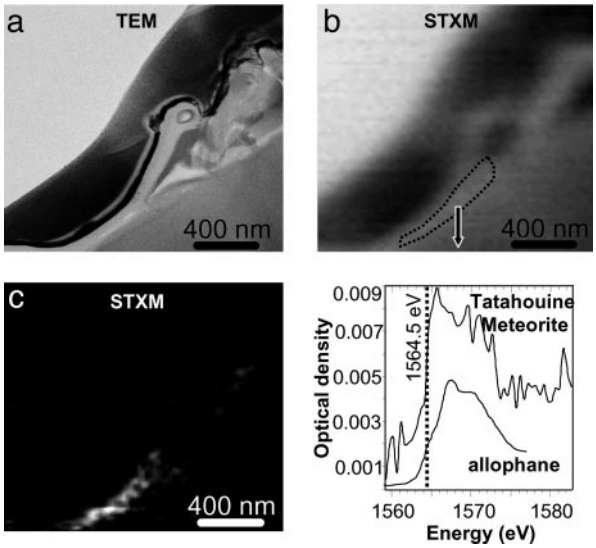

Fig. 3. Spectromicroscopy study of the microbe–mineral interface at the Al K-edge. (*A*) STXM image of the microorganism (same area as the one observed at the C edge; see Fig. 1) at 1,572 eV. (*B*) Corresponding TEM image. (*C*) Aluminum elemental map obtained from the subtraction of the images of the microorganism taken above and below the Al K-edge (at 1,572 and 1,560 eV, respectively), showing high enrichment in Al only beneath the microorganism. (*D*) Al K-edge NEXAFS spectrum from the Al-rich layer outlined in Fig. 2*A*, and reference spectrum of an allophane containing both four- and sixfold-coordinated Al (from ref. 28).

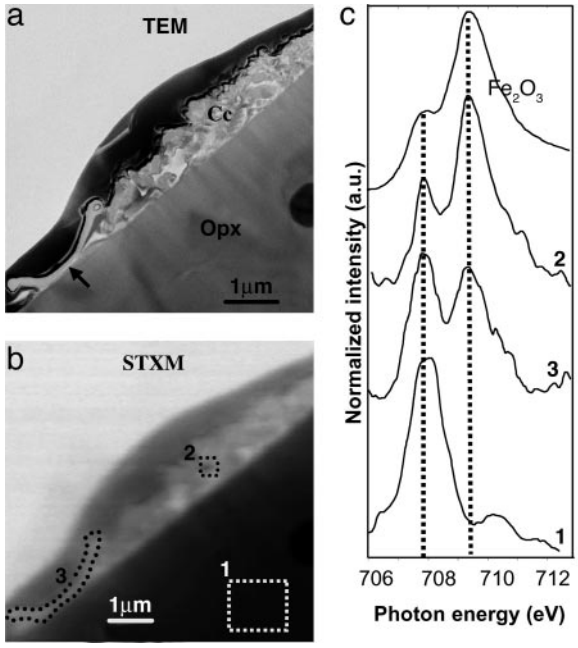

Fig. 4. Fe redox state analysis at the microbe–mineral interface. (*A*) TEM image of the cross section showing the microorganism (arrow), the calcite crystal cluster (Cc), and the orthopyroxene (Opx). (*B*) Equivalent STXM image at 707.8 eV. (*C*) Iron L_3-edge NEXAFS spectra from the pyroxene (area 1; see Fig. 2*B*), the calcite cluster (area 2), the microorganism (area 3), and reference hematite, representing the Fe^{3+} endmember. Dashed lines represent the positions of Fe L_3 maxima for Fe^{2+} and Fe^{3+} at 707.8 and 709.5 eV, respectively.

cluster (12, 15). We suggest that this microorganism uniquely coupled calcite precipitation and pyroxene dissolution by releasing molecules that mediated Ca-carbonate precipitation. In addition, we suggest that the same or other organic molecules enhanced pyroxene dissolution. A similar Urey-like reaction occurring in the presence of and promoted by microbes has been indicated by several studies (26, 27). Such microbially mediated reactions could be responsible for trapping some of the calcium and magnesium released by pyroxene dissolution as well as atmospheric CO_2 (2). The Urey reaction is classically considered to be a two-step reaction on a time scale of hundreds of thousands of years, with silicate weathering occurring on the continents and carbonate precipitation occurring in the oceans (2). Our results show that this reaction can take place on a very small scale over a much shorter time scale.

Aluminum Fate in a Microorganism Microenvironment. The same sample area was investigated by STXM imaging and NEXAFS microspectroscopy at the Al K-edge (1,560 eV; Fig. 3). By taking images below and above the Al K-edge, it was possible to obtain an Al distribution map (Fig. 3). This map shows that Al is preferentially concentrated beneath the microorganism. The Al coordination number in this 100-nm-thick layer was determined by acquiring an Al K-edge NEXAFS spectrum, which revealed an absorption edge position at 1,564.5 eV and a broad peak centered at ≈1,568 eV that are indicative of four- and sixfold-coordinated Al (28). This result is consistent with a disordered aluminosilicate, such as allophane (Fig. 3), and with TEM observations showing that the Al-rich layer is amorphous at the nanometer scale (15). Precipitation of clays at the surface of pyroxenes has been reported by several workers (e.g., see ref. 29). Our results indicate that the local concentration of Al is associated with the microorganism. One possible explanation for this association is that the microorganism reduces the water/solid ratio, which has been used to explain local reprecipitation of secondary products (30). This observation is also consistent with the finding that microorganisms can mediate the precipitation of aluminosilicates at their surface (31). Similar biologically induced microenvironments leading to localized etching and aluminosilicate precipitation have been found in altered oceanic volcanic glass by using optical microscopy (e.g., see ref. 32). In the present study, we observed the formation of an Al-rich layer only beneath the microorganism, which may impact the subsequent dissolution of the pyroxene. Indeed, such residual layers are potentially responsible for passivation of silicate surfaces and inhibition of further silicate dissolution (4, 33). In a Panglossian perspective, it is noted that the formation of this layer beneath rather than surrounding the microorganism provides a stable anchor substrate without preventing the microorganism from dissolving the neighboring substrate to take advantage of the release of essential nutrients from the pyroxene. It has also been suggested (P. C. Bennett, personal communication) that the formation of this Al-rich layer may be beneficial to the microorganism as it sequesters Al, which is a toxic metal and interferes with iron-chelating siderophores. Characterization of the trace element fluxes between this microorganism and the pyroxene substrate would be of great help in evaluating these suggestions.

Fe Oxidation at a Microorganism–Mineral Interface. Previous studies of the abiotic dissolution of Fe(II)-bearing pyroxene have revealed that Fe behavior is mostly controlled by redox conditions (33). Under oxic conditions at near neutral pH, which is likely the case for the Tatahouine pyroxene, Fe is oxidized, which may passivate the surface of the pyroxene (34). In contrast, under anoxic conditions, dissolution rates of Fe-pyroxenes are similar to those of Fe-free pyroxenes (33). To verify these earlier findings for dissolution of Fe-bearing pyroxenes under oxic conditions, we studied the Tatahouine sample at the Fe L_3-edge, which allowed us to determine the iron oxidation state (e.g., see ref. 35) in the microorganism–calcite–pyroxene microcosm at a

spatial resolution of <40 nm (Fig. 4). Iron spectra taken on the pyroxene (area 1) showed a major peak at 707.8 eV, indicative of Fe^{2+} (Fig. 4). Fe-rich particles in the calcite cluster (area 2) displayed a major peak at 709.5 eV, indicating that iron was oxidized after its release by dissolution of the pyroxene (Fig. 4). In the microorganism (area 3), however, the Fe L_3-edge shows a mixed iron valence (Fe^{2+} and Fe^{3+}) (Fig. 4). Spectra were recorded several times over a several hour period, and all were identical, indicating that beam damage was not responsible for this observation in area 3. One possible explanation for variable iron valence in and around the Tatahouine microorganism is that the iron oxidation state was modified by this microorganism, which creates a special microenvironment with a particular pO_2 and/or modifies the pH, resulting in slower oxidation of iron. Determining the taxonomy of the microorganism would help in verifying this hypothesis, although such identification of a single, partially fossilized microorganism, as in this case, would be extremely difficult. Another possibility is that organic molecules produced by the microorganism strongly bind dissolved Fe^{2+} and thus inhibit its oxidation as suggested by several previous studies (e.g., see ref. 36). Fe^{3+} is likely the stable form of iron at the surface of the Tatahouine sand. Whatever mechanisms are involved in iron redox behavior, the microorganism heavily impacts iron oxidation dynamics in a microenvironment, resulting in a major modification of pyroxene reactivity, compared with a purely abiotic environment. One consequence of the stabilization of Fe^{2+} is the delay of entrapment of the microorganism by Fe-oxides. Such stabilization could also provide a low-energy-cost iron source.

Summary and Conclusions

A filamentous microorganism appears to have had a major impact on the weathering of a meteoritic Fe^{2+}-Mg-orthopyroxene during some period of its 70 years of exposure in the southern Tunisian desert. Modifications of iron oxidation dynamics, calcium carbonate precipitation, and Al mobility by this microorganism may have resulted in different dissolution rates in regions surrounding the pyroxene separated by tens of nanometers. Our observations indicate that this microorganism coupled carbonate precipitation and pyroxene weathering, providing a potential sequestration mechanism for CO_2 and producing unique biosignatures in the form of rod-shaped nanocrystals of calcite. The ability to characterize this microorganism–calcium carbonate–pyroxene system at the sub-40-nanometer spatial scale by using STXM and TEM methods provides a unique view of how one type of microorganism controlled biomineral formation (e.g., see ref. 37) as well as orthopyroxene weathering in an arid environment. Although more systematic work on similar samples from various environments will be needed to understand the broader significance of the observations made here, the methodology presented in this paper should be helpful in assessing the importance of microorganisms in the evolution of Earth's surface chemistry and in identifying them in early Earth and planetary materials.

We thank the CP2M members in Marseille who granted access to the JEOL 2010F microscope and to the FEI Model 200 TEM FIB system, A. P. Hitchcock for providing reference C K-edge spectra for albumin and sodium alginate, Scott Fendorf (Stanford University) for a helpful review of this manuscript, and Phil Bennett and two anonymous reviewers for help in improving this article. The STXM studies were conducted on branch line 11.0.2.2 at the Advanced Light Source, which is supported by the Office of Science, Office of Basic Energy Sciences, Division of Materials Sciences, and Division of Chemical Sciences, Geosciences, and Biosciences of the U.S. Department of Energy at Lawrence Berkeley National Laboratory under Contract DE-AC03-76SF00098. This work was supported by National Science Foundation Grants CHE-0089215 (Stanford University Collaborative Research Activity in Environmental Molecular Science on Chemical and Microbial Interactions at Environmental Interfaces), CHE-0431425 (Stanford University Environmental Molecular Science Institute), and EAR-9905755. K.B. thanks the French Foreign Ministry for a Lavoisier Fellowship.

1. Marschner, H. (1995) *The Mineral Nutrition of Higher Plants* (Academic, London).
2. Berner, R. A. (1995) *Rev. Mineral.* **31,** 565–583.
3. Rothman D. H. (2001) *Proc. Natl. Acad. Sci. USA* **98,** 4305–4310.
4. Brantley, S. L. & Chen, Y. (1995) *Rev. Mineral.* **31,** 119–172.
5. Oelkers, E. H. & Schott, J. (2001) *Geochim. Cosmochim. Acta* **65,** 1219–1231.
6. White, A. F. & Brantley, S. L. (2003) *Chem. Geol.* **202,** 479–506.
7. Brantley, S. L., Liermann, L. J., Guynn, R. L., Anbar, A., Icopini, G. A. & Barling, J. (2004) *Geochim. Cosmochim. Acta* **68,** 3189–3204.
8. Barker, W. W., Welch, S. A. & Banfield, J. F. (1997) *Rev. Mineral.* **35,** 391–428.
9. Little, B. J., Wagner, P. A. & Lewandowski, Z. (1995) *Rev. Mineral.* **35,** 123–159.
10. Liermann, L. J., Kalinowski, B. E., Brantley, S. L. & Ferry, J. G. (2000) *Geochim. Cosmochim. Acta* **64,** 587–602.
11. Santelli, C. M., Welch, S. A., Westrich, H. R. & Banfield, J. F. (2001) *Chem. Geol.* **180,** 99–115.
12. Benzerara, K., Menguy, N., Guyot, F., Dominici, C. & Gillet, P. (2003) *Proc. Natl. Acad. Sci. USA* **100,** 7438–7442.
13. Barrat, J. A., Gillet, P., Lesourd, M., Blichert-Toft, J. & Poupeau, G. R. (1999) *Meteorit. Planet. Sci.* **34,** 91–97.
14. Barrat, J. A., Gillet, P., Lecuyer, C., Sheppard, S. M. F. & Lesourd, M. (1998) *Science* **280,** 412–414.
15. Benzerara K., Menguy, N., Guyot, F., Vanni, C. & Gillet, P. *Geochim. Cosmochim. Acta*, in press.
16. Heaney, P. J., Vicenzi, E. P., Giannuzzi, L. A. & Livi, K. T. V. (2001) *Am. Mineral.* **86,** 1094–1099.
17. Tyliszczak, T., Warwick, T., Kilcoyne, A. L. D., Fakra, S., Shuh, D. K., Yoon, T. H., Brown, G. E., Jr., Andrews, S., Chembrolu V., Strachan, J. & Acremann, Y. (2004) *AIP Conf. Proc.* **705,** 1356–1359.
18. Yoon, T. H., Johnson, S. B., Doyle, C. S., Benzerara, K., Tyliszczak, T., Shuh, D. K. & Brown, G. E., Jr. (2004) *Langmuir* **20,** 10361–10366.
19. Lawrence, J. R., Swerhone, G. D. W., Leppard, G. G., Araki, T., Zhang, X., West, M. M. & Hitchcock, A. P. (2003) *Appl. Environ. Microbiol.* **69,** 5543–5554.
20. Myneni, S. C. B. (2002) *Rev. Mineral. Geochem.* **49,** 485–579.
21. Kirkland, B. L., Lynch, F. L., Rahnis, M. A., Folk, R. L., Molineux, I. J. & McLean, R. J. C. (1999) *Geology* **27,** 347–350.
22. Arp, G., Reimer, A. & Reitner, J. (2003) *J. Sediment. Res.* **73,** 105–127.
23. Weiner, S. & Addadi, L. (1997) *J. Mater. Chem.* **7,** 689–702.
24. Aizenberg, J., Lambert, G., Weiner, S. & Addadi, L. (2002) *J. Am. Chem. Soc.* **124,** 32–39.
25. Wogelius, R. A. & Walther, J. V. (1991) *Geochim. Cosmochim. Acta* **55,** 943–954.
26. Ferris, F. G., Wiese, R. G. & Fyfe, W. S. (1994) *Geomicrobiol. J.* **12,** 1–13.
27. Roberts, J. A., Bennett, P. C., Gonzalez, L. A., Macpherson, G. L. & Milliken, K. L. (2004) *Geology* **32,** 277–280.
28. Ildefonse, P., Kirkpatrick, R. J., Montez, B., Calas, G., Flank, A. M. & Lagarde, P. (1994) *Clays Clay Miner.* **42,** 112–121.
29. Banfield, J. F., Barker, W. W., Welch, S. A. & Taunton, A. (1999) *Proc. Natl. Acad. Sci. USA* **96,** 3404–3411.
30. Casey, W. H., Westrich, H. R., Banfield, J. F., Ferruzzi, G. & Arnold, G. W. (1993) *Nature* **366,** 252–256.
31. Ueshima, M. & Tazaki, K. (2001) *Clays Clay Miner.* **49,** 292–299.
32. Fisk, M. R., Giovannoni, S. J. & Thorseth, I. H. (1998) *Science* **281,** 978–980.
33. Schott, J. & Berner, R. A. (1983) *Geochim. Cosmochim. Acta* **47,** 2233–2240.
34. Siever, R. & Woodford, N. (1979) *Geochim. Cosmochim. Acta* **43,** 717–724.
35. Peng, G., Van Elp, J., Jang, H., Que, L., Armstrong, W. H. & Cramer, S. P. (1995) *J. Am. Chem. Soc.* **117,** 2515–2519.
36. Neubauer, S. C., Emerson, D. & Megonigal, J. P. (2002) *Appl. Environ. Microbiol.* **68,** 3988–3995.
37. Chan, C. S., De Stasio, G., Welch, S. A., Girasole, M., Frazer, B. H., Nesterova, M. V., Fakra, S. & Banfield, J. F. (2004) *Science* **303,** 1656–1658.